Fast algebra algorithm of shape-from-shading with specular reflectance

Lei Yang (杨 磊) and Jiuqiang Han (韩九强)

School of Electronics and Information Engineering, Xi'an Jiaotong University, Xi'an 710049

Received September 12, 2006

Shape-from-shading (SFS) is to reconstruct three-dimensional (3D) shape from a single gray image, which is an important problem in computer vision. We propose a novel SFS method based on hybrid reflection model which contains both diffuse reflectance and specular reflectance. The intensity gradient of image is in the direction that the shape of surface changes most, so we use directional derivative of the reflectance map as parts of objective function. When discrete characteristic of digital images is considered, finite difference approximates differential operator. So the reflectance map equation described by a partial differential equation (PDE) turns into an algebra equation about the unknown surface height correspondingly. Using iterative numeric computation, a new SFS method is gained. Experiments on synthesis and real images show that the proposed SFS method is accurate and fast.

OCIS codes: 110.6150, 100.5010.

Shape-from-shading (SFS) is a classical problem in computer vision, which reconstructs the three-dimensional (3D) shape from one two-dimensional (2D) image[1−3]. The brightness of image points mainly depends on four respects: the orientation of light source, the location of camera, the orientation (shape) of object and the reflectance property of its surface[4]. SFS is based on the reflectance map equation at each imaged pixel. The development of SFS mainly depends on two aspects, namely the research of a better reflectance model and the investigation of an effective SFS algorithm. The classical formulation of SFS is based on Lambertian reflectance model together with the minimization of the total error function using the calculus of variations[2,3]. Comprehensive survey of SFS can be found in Refs. [2,5]. Recent reconstruction methods use advanced computation tools such as neural networks[4,6,7], viscosity solution of partial differential equation (PDE)[8], level set approach[9], and so on. SFS has been widely applied in terrain analysis for moon and ocean, medical imaging, industry automatic inspection, etc.[1,10,11].

A fast SFS method based on hybrid reflection model is proposed in this paper. We used the hybrid reflection model because it is more prone to real reflectance than Lambertian model or Torrance-Sparrow model[4]. We mainly make progress in the objective function containing gradient of image and effective reconstruction method. The intensity gradient is in the direction that the shape of surface changes most, so we decide to use directional derivative of image as parts of objective function in our SFS. When discrete characteristic of digital images is considered, finite difference approximates differential operator. So the reflectance map equation described by PDE turns into an algebra equation about the unknown surface height. Using iterative numeric computation, a new SFS method can be gained.

In SFS, we generally assume a point light source located in infinite location. E denotes the light strength, and its direction is $\vec{n}_{\rm i} = (-p_0, -q_0, 1)^{\rm T}$ in image center coordinate. The observing camera is located in direction of $\vec{n}_{\rm o} = (0, 0, 1)^{\rm T}$. The surface is $z = z(x, y)$, and its direction is $\vec{n}$ ($\vec{n} = (-\frac{\partial z}{\partial x}, -\frac{\partial z}{\partial y}, 1)^{\rm T}$). Orthogonal projection is used in the procedure of imaging. Two classes of reflection models, namely, diffuse reflection and specular reflection, are usually considered. For most SFS algorithms, the reflectance model is assumed to be a Lambertian one[2]. The reflectance map function of the surface illuminated by single point light source is given by

$$R_{\rm d}(\vec{n}, \vec{n}_{\rm i}, \vec{n}_{\rm o}) = \frac{E}{\pi|\vec{n}||\vec{n}_{\rm i}|} \times \vec{n}^{\rm T} \cdot \vec{n}_{\rm i}. \tag{1}$$

On the other hand, Torrance-Sparrow model using a Gaussian distribution to model the facet orientation function is used to deal with specular reflectance phenomena[4]. Another simple specular model is Phong's model[7] which indicates that the light perceived by the camera is represented as

$$R_{\rm s}(\vec{n}, \vec{n}_{\rm i}, \vec{n}_{\rm o}) = E \times (\vec{n}^{\rm T} \cdot \vec{n}_{\rm spec})^K, \tag{2}$$

where the vector $\vec{n}_{\rm spec} = (\vec{n}_{\rm i} + \vec{n}_{\rm o})/\left|\vec{n}_{\rm i} + \vec{n}_{\rm o}\right|$ is called the halfway-vector (or specular reflectance direction), and K denotes a constant. Different values of K denote different kinds of surfaces which are more or less mirror-like.

But real surface reflectance is neither pure Lambertian nor pure specular. Instead, they are a combination of diffuse and specular components. Tagare *et al.* proposed a hybrid model consisting of three components[12]. A linear combination model of diffuse and specular components described by Gaussian function was used by Cho[4]. We use the hybrid reflectance as[7]

$$R(p, q) = (1 - w)R_{\rm d}(p, q) + wR_{\rm s}(p, q), \tag{3}$$

where $p(x, y) = -\frac{\partial z(x,y)}{\partial x}$ and $q(x, y) = -\frac{\partial z(x,y)}{\partial y}$ denote the x- and y-partial derivatives of reconstructed 3D surface height $z = z(x, y)$ with respect to the image coordinates x and y, respectively, $\vec{n}_{\rm spec}$ denoted as $(-p_h, -q_h, 1)^{\rm T}$ is specular reflectance direction, and $w \in [0, 1]$ is the factor of specular component. When gray values of image and reflectance function are both normalized, we get the well-known reflectance map equa-

tion

$$(1-w)\frac{pp_0+qq_0+1}{\sqrt{p^2+q^2+1}\sqrt{p_0^2+q_0^2+1}}$$

$$+w(\frac{pp_h+qq_h+1}{\sqrt{p^2+q^2+1}\sqrt{p_h^2+q_h^2+1}})^K=\frac{I(x,y)-I_{\min}}{I_{\max}-I_{\min}}, \quad (4)$$

where $I_{\max}$ and $I_{\min}$ are the acquired maximum and minimum intensities of image $I(x,y)$.

We will solve Eq. (4) associating the image brightness. The direction of intensity gradient is the direction in which the shape of the surface changes most[13]. We notice that the gradient of image describes the detail of original surface, so directional derivative of the image can be used to deal with SFS problem. The direction of gradient is denoted by

$$I_x=\frac{\partial I}{\partial x}=\frac{\partial R}{\partial p}\frac{\partial p}{\partial x}+\frac{\partial R}{\partial q}\frac{\partial q}{\partial x},$$

$$I_y=\frac{\partial I}{\partial y}=\frac{\partial R}{\partial p}\frac{\partial p}{\partial y}+\frac{\partial R}{\partial q}\frac{\partial q}{\partial y}. \quad (5)$$

When index (i,j) in discrete domain approximates index (x,y) in continuous domain, the PDE Eq. (4) in continuous domain can be written as an algebra equation as

$$R(p_{i,j},q_{i,j})=I(i,j). \quad (6)$$

The objective function we used can be described as

$$R(p_{i,j},q_{i,j})+\alpha(R_x(p_{i,j},q_{i,j})+R_y(p_{i,j},q_{i,j}))$$

$$=I(i,j)+\alpha(I_x(i,j)+I_y(i,j)), \quad (7)$$

where $I(i,j)$ is the digital image brightness, $I_x(i,j)$ and $I_y(i,j)$ are the gradients of image along x- and y-direction. Our experiments and analysis result show that more error may be caused if gradients of image are used directly, because they may introduce high-frequency noise. On the other hand, gradient of image describes the detail of image as we analyzed. So we use a positive factor α ($\alpha\geq 0$) to balance this contradiction. Center difference is used to approximate differential operator, namely

$$p(x,y)\approx p_{i,j}=\frac{z_{i+1,j}-z_{i-1,j}}{2},$$

$$q(x,y)\approx q_{i,j}=\frac{z_{i,j+1}-z_{i,j-1}}{2},$$

$$\frac{\partial p}{\partial x}\approx\frac{p_{i+1,j}-p_{i-1,j}}{2}=\frac{z_{i+2,j}-2z_{i,j}+z_{i-2,j}}{4},$$

$$\frac{\partial q}{\partial y}\approx\frac{q_{i,j+1}-q_{i,j-1}}{2}=\frac{z_{i,j+2}-2z_{i,j}+z_{i,j-2}}{4},$$

$$\frac{\partial p}{\partial y}=\frac{\partial q}{\partial x}\approx\frac{p_{i,j+1}-p_{i,j-1}}{2}$$

$$=\frac{z_{i+1,j+1}-z_{i-1,j+1}-z_{i+1,j-1}+z_{i-1,j-1}}{4},$$

$$I_x(i,j)=\frac{I(i+1,j)-I(i-1,j)}{2},$$

$$I_y(i,j)=\frac{I(i,j+1)-I(i,j-1)}{2}. \quad (8)$$

Subsitute Eq. (8) into Eq. (7), after rearranging we get

$$F(z_{i-2,j},z_{i-1,j},z_{i+1,j},z_{i+2,j},z_{i,j-2},z_{i,j-1},z_{i,j},$$

$$z_{i,j+1},z_{i,j+2},z_{i-1,j-1},z_{i-1,j+1},z_{i+1,j-1},z_{i+1,j+1})=0. \quad (9)$$

The form of F in Eq. (9) is as follows. For Lambertian reflectance, differential of $R_{\rm d}(p,q)$ is

$$A=\frac{\partial R_{\rm d}}{\partial p}=\frac{1}{\sqrt{p_0^2+q_0^2+1}}(\frac{p_0(q^2+1)-(q_0q+1)p}{\sqrt{(p^2+q^2+1)^3}}), \quad (10a)$$

$$B=\frac{\partial R_{\rm d}}{\partial q}=\frac{1}{\sqrt{p_0^2+q_0^2+1}}(\frac{q_0(p^2+1)-(p_0p+1)q}{\sqrt{(p^2+q^2+1)^3}}). \quad (10b)$$

Rearranging Eq. (7) as

$$F=R(p_{i,j},q_{i,j})+\alpha(R_x(p_{i,j},q_{i,j})+R_y(p_{i,j},q_{i,j}))$$

$$-I(i,j)-\alpha(I_x(i,j)+I_y(i,j))=0, \quad (11)$$

using Eqs. (8), (10), and (11), then we have

$$F(z_{i-2,j},z_{i-1,j},z_{i+1,j},z_{i+2,j},z_{i,j},z_{i,j-2},z_{i,j-1},$$

$$z_{i,j+1},z_{i,j+2},z_{i-1,j-1},z_{i-1,j+1},z_{i+1,j-1},z_{i+1,j+1})$$

$$=\frac{1}{\sqrt{p_0^2+q_0^2+1}}$$

$$\times\frac{(z_{i+1,j}-z_{i-1,j})p_0+(z_{i,j+1}-z_{i,j-1})q_0+2}{\sqrt{(z_{i+1,j}-z_{i-1,j})^2+(z_{i,j+1}-z_{i,j-1})^2+4}}$$

$$+\alpha(\frac{A}{4}(z_{i+2,j}-2z_{i,j}+z_{i-2,j})$$

$$+(\frac{A+B}{4})(z_{i+1,j+1}-z_{i-1,j+1}-z_{i+1,j-1}+z_{i-1,j-1})$$

$$+\frac{B}{4}(z_{i,j+2}-2z_{i,j}+z_{i,j-2}))$$

$$-I(i,j)-\alpha(I_x(i,j)+I_y(i,j))=0. \quad (12)$$

For hybrid reflectance, similar with Eq. (12) but slight

difference as A, B is substituted by A', B', where

$$A' = \frac{\partial R}{\partial p} = (1-w)A$$

$$+wK \times R_{\rm s}^{K-1} \frac{1}{\sqrt{p_h^2+q_h^2+1}} \left(\frac{p_h(q^2+1)-(q_h q+1)p}{\sqrt{(p^2+q^2+1)^3}}\right), \tag{13a}$$

$$B' = \frac{\partial R}{\partial q} = (1-w)B$$

$$+wK \times R_{\rm s}^{K-1} \frac{1}{\sqrt{p_h^2+q_h^2+1}} \left(\frac{q_h(p^2+1)-(p_h p+1)q}{\sqrt{(p^2+q^2+1)^3}}\right). \tag{13b}$$

The following deduction is the same as that of Lambertian reflectance. General iterative formulation is shown as $z_{i,j} = z_{i,j} + \mu \times F$. By solving Eq. (12) using general iterative algorithm, a new iterative SFS algorithm is obtained as

$$z_{i,j}^{(k+1)} = z_{i,j}^{(k)}$$

$$+\mu \times F(z_{i-2,j}^{(k)}, z_{i-1,j}^{(k)}, z_{i+1,j}^{(k)}, z_{i+2,j}^{(k)}, z_{i,j-2}^{(k)}, z_{i,j-1}^{(k)}, z_{ij}^{(k)},$$

$$z_{i,j+1}^{(k)}, z_{i,j+2}^{(k)}, z_{i-1,j-1}^{(k)}, z_{i-1,j+1}^{(k)}, z_{i+1,j-1}^{(k)}, z_{i+1,j+1}^{(k)}), \tag{14}$$

where $k = 1, 2, \cdots$ denote the iterative times, and μ is iterative rate. The computation stops when iterative time limitation is arrived or error criteria are satisfied.

We performed two experiments to evaluate the performance of the proposed SFS method. One is to compare the result of the proposed SFS method with existing classical ones using synthesized image of hemisphere produced by hybrid reflectance model. The other is about a real image of metal statuary of Xuesen Qian which witch containing specular reflectance captured in Xi'an Jiaotong University using CANNON (CCD) camera. All the algorithms are realized under the following conditions: AMD 1.7-GHz CPU, 256 MB RAM, Windows 2000, and Matlab7.0.

The reconstructed height of surface is denoted by $z_{i,j}$, and $z_{i,j}^0$ is original height of surface. Main comparing criteria of difference between them are mean error (ME) and mean squared root error (MS) defined as

$$\text{ME} = \frac{1}{M \times N} \sum_{i=1}^{M} \sum_{j=1}^{N} (z_{i,j} - z_{i,j}^0),$$

$$\text{MS} = \sqrt{\frac{\sum_{i=1}^{M} \sum_{j=1}^{N} (z_{i,j} - z_{i,j}^0)^2}{M \times N}}, \tag{15}$$

where $M \times N$ is the number of pixels of digital image.

Figure 1(a) shows the image of a synthesized hemisphere[4]

$$z(x,y) = \begin{cases} \sqrt{40^2 - x^2 - y^2} & \text{if } x^2+y^2 \le 40^2 \\ 0 & \text{otherwise} \end{cases} \tag{16}$$

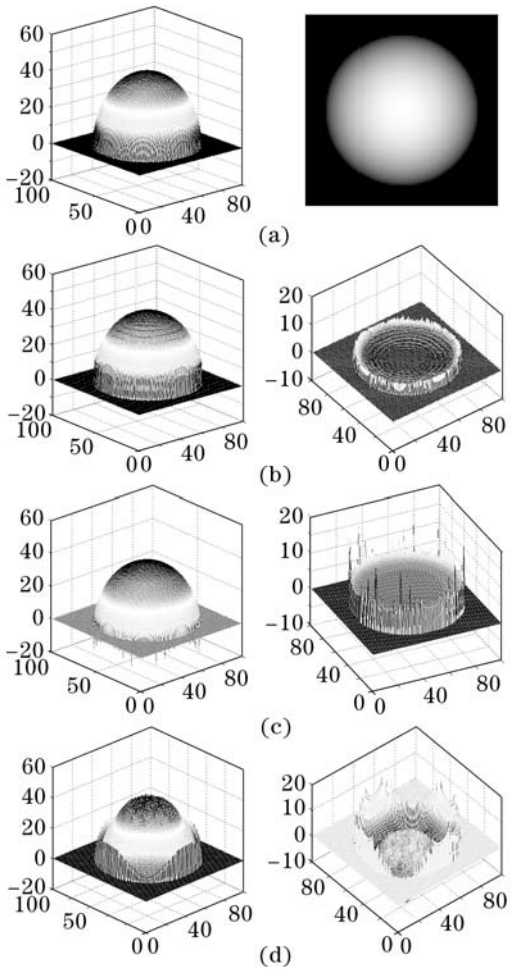

Fig. 1. Reconstruction result of synthesized hemisphere. (a) Shape (left) and image (right) of synthesized hemisphere; (b)—(d) reconstructed shapes (left) and errors (right) using the proposed method, Kimmel's method, and Horn's method.

Table 1. Comparing Result of Reconstructed Shape of Synthesized Hemisphere

	Proposed Method	Kimmel's[9]	Horn's[2]
ME of Height	0.9806	3.1341	−3.7891
MS of Height	1.4110	5.0887	5.4277
CPU Time (s)	82.2780	120.1200	306.3910

produced by hybrid reflectance. The light is located in the direction $(0,0,1)^{\rm T}$. K and w in Eq. (3) are selected as 10 and 0.3, respectively. The number of pixels of image $M \times N$ is 100×100. We use camera center coordinates. Reconstructed surface and errors with the original hemisphere using proposed SFS method are shown as Fig. 1(b). Figures 1(c) and (d) are two reconstruction results using Kimmel's method[9] and the classical method proposed by Horn[2] for comparison. The numeric comparing results using the proposed method, Ron's and Horn's method illuminated in Fig. 1 are listed in Table 1. In our algorithm, iterative rate μ is 0.1, the factor α is 0.11, the iterative times is 200.

Figure 2(a) shows an image of metal statuary of Xuesen Qian after nine-neighbor mean filtering. Figures 2(b),

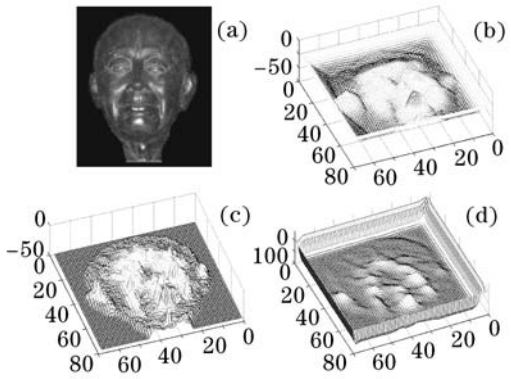

Fig. 2. Reconstruction results of real image of a metal statuary. (a) Filtered image; (b)—(d) reconstruction results using the proposed method, Kimmel's method, and Horn's method.

(c) and (d) are the reconstruction results using the proposed method, Kimmel's method and Horn's method under same iterative condition. In our algorithm, iterative rate μ is 0.05, the factor α is 0.1. The iterative times of three methods are 300, and K, w in Eq. (3) are selected as 20 and 0.3, respectively. The number of pixels of image is 70×80. The light source is the flash light of the camera, so the direction of light is $(0, 0, 1)^{\mathrm{T}}$ approximately.

Experiments indicate that the proposed SFS method is an accurate and fast 3D shape reconstruction algorithm. The synthesis experiment shows that the proposed method is more accurate and faster than the other two methods. The experiment on real image illuminated that SFS with real specular component is a difficult work. In our method, the main error lies in big reflectance angle. The error of reconstructed shape is mainly located in specular reflectance because acquired image should describe highlight correctly. But in real situation, ideal condition of image form is difficult to satisfy. Two possible reasons are unideal point light source and unsuitable reflectance model.

In conclusion, a novel discrete SFS method based on hybrid reflection model is proposed. Hybrid reflectance model is used because they are prone to reality. We use directional derivative of image and reflectance map equation as objective function. When discrete characteristic of digital images is considered, central-finite difference approximates differential operator. The reflectance map equation described by a PDE turns into an algebra equation about the unknown height. Using iterative numeric computation, the unknown surface height is calculated. Experiments on synthesis and real images show that the proposed SFS method is accurate and fast. Further study of SFS includes the more accurate reconstruction methods and their convergence and speed. Color SFS is also an interesting investigation direction.

This work was supported by the National Natural Science Foundation of China under Grant No. 60502021. L. Yang's e-mail address is yangyoungya@sina.com.

References

1. B. K. P. Horn, in P. H. Winston, (ed.) *The Psychology of Computer Vision* (McGraw-Hill, New York, 1975) Chap.4, pp.115—155.
2. B. K. P. Horn, Int. J. Computer Vision **5,** 37 (1990).
3. R. Zhang, P.-S. Tsai, J. E. Cryer, and M. Shah, IEEE Trans. Pattern Analysis and Machine Intelligence **21,** 690 (1999).
4. S.-Y. Cho and T. W. S. Chow, Neural Computation **14,** 2751 (2002).
5. J.-D. Durou, M. Falcone, and H. Sagona, IRIT Research Report 2004-2-R (2004).
6. Y. Hu, B. Liu, F. Li, and C. Meng, Acta Photon. Sin. (in Chinese) **32,** 985 (2003).
7. C.-T. Lin, W.-C. Cheng, and S.-F. Liang, IEEE Trans. Neural Networks **16,** 1601 (2005).
8. A. Tankus, N. Sochen, and Y. Yeshurun, Int. J. Computer Vision **63,** 21 (2005).
9. R. Kimmel and J. A. Sethian, J. Mathematical Imaging and Vision **14,** 237 (2001).
10. L. Song, X. Qu, K. Xu, and L. Lu, NDT&E International **38,** 381 (2005).
11. A. G. Bors, E. R. Hancock, and R. C. Wilson, IEEE Trans. Pattern Analysis and Machine Intelligence **25,** 974 (2003).
12. H. D. Tagare and R. J. P. deFigueiredo, IEEE Trans. Pattern Analysis and Machine Intelligence **13,** 133 (1991).
13. R. Zhang and M. Shah, IEEE Trans. Systems, Man, and Cybernetics A **29,** 318 (1999).